Supramolecular Chemistry
Publication details, including instructions for authors and subscription information:
http://www.informaworld.com/smpp/title~content=t713649759

Observation of Transient Alkali Metal Inclusion in Oxacalix[3]arenes

Mijan Miah[a]; Karl D. Pavey[a]; Vladimir M. Gun'ko[b]; Rosemary Sheehan[a]; Peter J. Cragg[a]
[a] School of Pharmacy and Biomolecular Sciences, University of Brighton, Brighton, UK [b] Institute of Surface Chemistry, Kiev, Ukraine

To cite this Article Miah, Mijan , Pavey, Karl D. , Gun'ko, Vladimir M. , Sheehan, Rosemary and Cragg, Peter J.(2004) 'Observation of Transient Alkali Metal Inclusion in Oxacalix[3]arenes', Supramolecular Chemistry, 16: 3, 185 — 192
To link to this Article: DOI: 10.1080/10610270310001644473
URL: http://dx.doi.org/10.1080/10610270310001644473

Supramolecular Chemistry, April 2004, Vol. 16 (3), pp. 185–192

Taylor & Francis
Taylor & Francis Group

Observation of Transient Alkali Metal Inclusion in Oxacalix[3]arenes

MIJAN MIAH[a], KARL D. PAVEY[a], VLADIMIR M. GUN'KO[b], ROSEMARY SHEEHAN[a] and PETER J. CRAGG[a,*]

[a]*School of Pharmacy and Biomolecular Sciences, University of Brighton, Brighton BN2 4GJ, UK;* [b]*Institute of Surface Chemistry, 17 General Naumov Street, 03164 Kiev, Ukraine*

Received (in Southampton, UK) 14 October 2003; Accepted 27 October 2003

Oxacalix[3]arenes exhibit transient binding to Na^+, K^+ and Ca^{2+}, with a strong preference for Na^+, as determined by a quartz crystal resonant sensor technique. Computational models for the behaviour indicate that the preference for Na^+ is due to the depth to which that cation is drawn into the macrocycle's central cavity.

Keywords: Calixarene; Metal binding; Sensor; Computer simulation

INTRODUCTION

The inclusion chemistry of calixarenes has been studied for many years, primarily by X-ray crystallographic and NMR techniques, to reveal how small molecules and ions are held within the macrocycles' cavities. From simple host–guest complexes [1–3] to extensive supramolecular assemblies [4–6], the calixarene framework never fails to generate new insights into molecular interactions, with relevance to fields as diverse as sensor technology [7] and enzyme mimicry [8]. We have been investigating the chemistry of a sub-group of the calixarenes, the oxacalix[3]arenes [9,10] (**1**; see Fig. 1), which contain *para*-substituted phenolic and ethereal binding domains, exhibit threefold symmetry and may be derivatized through either the upper or the lower rim to expand their capabilities for molecular recognition [11–16]. Both crystallographic [17–19] and NMR techniques [20] reveal that the threefold symmetry element is influential in the range of neutral and cationic organic guests attracted to the macrocyclic cavity; however, symmetry is less important in the complexation of metal cations. Experiments based on picrate extraction by **1a** indicate little selectivity between the alkali metal cations [21], whereas **1b** forms a stable complex with Na^+. Our interest in calixarene inclusion phenomena was sparked by the discovery that Na^+, in competition with K^+, Mg^{2+} and Ca^{2+}, is selectively transported across a cell membrane by **1b** and that the complex, in the solid state, contains two Na^+ binding domains [22]. One cation interacts weakly with the upper cavity of the oxacalix[3]arene and is linked by a water molecule to a second cation that is held strongly by the lower rim diethylacetamide substituents.

Na^+ binding to calixarenes derivatized with diethylacetamide moieties on their lower rims has long been recognized [23–25]; however, we believe that the upper binding site in **1b**, with its potential cation–π interactions, may be the source of the metal's initial attraction to the macrocycle prior to falling into the trap set by preorganized lower rim substituents. We assume that Na^+ is initially attracted to the macrocyclic "funnel" *before* being drawn into the lower binding region because if it were attracted primarily to the amide groups, the cation would be expected to bind in an *exo*-fashion. Such a binding mode is seen in the structure of $(\mathbf{1b}{\cdot}HgCl_2)_2$ [26].

In the absence of the lower binding site do oxacalix[3]arenes still show a preference for Na^+ through a dynamic process that is not revealed by extraction experiments? To test this hypothesis we have used a combination of real-time binding assays (the quartz crystal resonant sensor or QCRS),

*Corresponding author. Tel.: +44-127-364-2037. Fax: +44-127-367-9333. E-mail: p.j.cragg@bton.ac.uk

ISSN 1061-0278 print/ISSN 1029-0478 online © 2004 Taylor & Francis Ltd
DOI: 10.1080/10610270310001644473

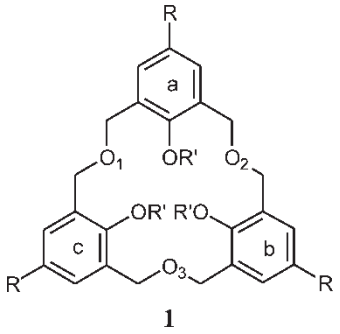

1

1a R = *t*-butyl R' = H

1b R = *t*-butyl R' =

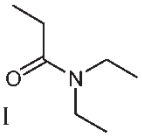

1c R = CO_2Et R' = H

FIGURE 1 Oxacalix[3]arenes **1a**–**c** with ethereal oxygens and ring centroids identified.

previously used to measure small molecule–DNA interactions [27,28], among many applications [29–31], and computational techniques.

EXPERIMENTAL

Materials

All materials and solvents were from Sigma-Aldrich (Gillingham, Dorset, UK), unless stated otherwise. Oxacalix[3]arenes **1a** and **1b** were prepared as described in the literature [32,33]. NMR spectra were recorded on a Bruker AM-360 at 360 and 90 MHz for ^1H and ^{13}C, respectively. Chemical shifts were referenced to tetramethylsilane (TMS). MALDI-TOF mass spectra were recorded on a Kratos PC Kompact (Kratos, UK) using a Co ultrafine powder (Co-UFP) ionizing matrix. Infrared spectra were recorded using a Perkin Elmer 1600 series FTIR with a diamond diffraction sample holding system. Compounds were deemed to be pure based on NMR analysis.

Synthesis

Preparation of Ethyl 3,5-Bis(hydroxymethyl)-4-hydroxybenzoate

Ethyl 4-hydroxybenzoate (25 g, 0.15 mol) was dissolved in cold aqueous NaOH (60 ml, 12% solution) and condensed with aqueous formaldehyde (32 ml, 37% solution) for 72 h at 55°C. After cooling to room temperature, the vigorously stirred solution was neutralized using a 15% solution of acetic acid, resulting in the formation of a yellow oil. The oil was extracted three times using diethyl ether and the ether extract dried using anhydrous sodium sulphate. The solution was filtered and the ether removed under reduced pressure to yield a pale yellow tar. The tar was dissolved in a minimum of hot acetone, cooled to −10°C for 12 h and filtered to give the title compound as a white or very pale yellow solid. Yield: 20.4 g (60%); mp 122.0–123.2°C (lit. 139°C, from benzene/petroleum ether [34]); ^1H NMR (methanol-d_4) δ 7.85 (s, 2H, Ar–H), 4.87 (s, 4H, $-CH_2OH$), 4.27 (q, 2H, $-CH_2-$), 1.36 (t, 3H, $-CH_3$); ^{13}C NMR (methanol-d_4) δ 170.30, 134.66, 131.61, 130.40, 124.88, 63.72, 32.65, 22.74; IR ν 3417.5, 3176.5, 2975.6, 2945.5, 2915.4, 2875.2, 1684.4, 1604.1, 1202.3, 1006.5 and 765.5 cm^{-1}; MS *m/z* 248.5 ($M + Na^+$).

7,15,23-Triethylacetoxy-25,26,27-trihydroxy-2,3,10,11,18,19-hexahomo-3,11,19-trioxacalix[3]arene (1c) [35]

Ethyl 3,5-bis(hydroxymethyl)-4-hydroxybenzoate (25 g, 0.11 mol) was refluxed in *o*-xylene (100 ml) with *p*-toluenesulphonic acid (2.09 g, 0.01 mol) for 4 h under N_2 using a Dean–Stark apparatus. The solvent was removed under reduced pressure and diethyl ether (20 ml) was added to extract included *o*-xylene from the product. The solvent was again removed under reduced pressure and the resulting white solid dissolved in a minimum of dichloromethane. Methanol was added until the solution became cloudy. Cooling to −10°C for 12 h precipitated **1c** as a white solid. Yield: 7.2 g (30%); mp 229.6–231.7°C; ^1H NMR ($CDCl_3$) δ 9.2 (s, 3H, Ar–OH), 7.87 (s, 6H, Ar–H), 4.77 (s, 12H, $-OCH_2-$), 4.33 (q, 6H, $-CH_2-$), 1.39 (t, 9H, $-CH_3$); ^{13}C NMR ($CDCl_3$) δ 165.99, 160.01, 131.46, 128.84, 123.79, 70.78, 60.64, 29.51; IR ν 3397.4, 3317.1, 2975.6, 2915.4, 2855.1, 1717.0, 1608.4, 1315.4, 1197.3, 1076.8, 1031.6 and 765.5 cm^{-1}; MS *m/z* 623.3 (M^+).

Procedure for Quartz Crystal Resonant Sensor (QCRS) Experiments

Quartz crystal blanks (8.6 mm diameter, 10 MHz, Spartan Europe, Portsmouth, UK), furnished on both faces with gold electrodes (100 nm thickness, 5 mm diameter), were mounted in novel PEEK™ cartridges (pat. pending # GB 0019340.9) prior to insertion into a custom-built flow injection system (pat. pending # GB 0019336.7). Crystal oscillation was achieved using a novel oscillation circuit based upon auto gain control technologies designed to give extremely high

oscillation capabilities with very low noise under high liquid loading (pat. # WO 00/25118). Real-time crystal oscillation data and other circuit parameters were recorded with respect to time by way of a custom-written Labview™ application (National Instruments, Newbury, UK) at a resolution of 1 s. Liquid flow through the crystal flow cell was achieved using a Shimadzu LC-9A dual piston HPLC pump with all experiments carried out at a flow rate of 5 μl min^{-1}. Introduction of sample and ligand was through an all-PEEK™ Rheodyne™ MBB pulseless six-way injection valve fitted with a 20-μl loop via a Gilson 235 autoinjector. Water-cooled Peltier heaters allowed all experiments to be carried out at 25 ± 0.1°C. Gold sensor electrodes were coated with injections of the 11-mercaptoundecanoic acid (1 mM in ethanol, stabilized over 24 h) using established thiol–gold interaction chemistry [36]. Crystals were placed in the flow chamber and a 5 μl min^{-1} flow of 18 MΩ HPLC-grade H_2O initiated. Upon observation of baseline stability reaching ±0.2 Hz or better, sequential injections of oxacalix[3]arene (prepared as saturated aqueous solutions of **1a** or **1c**, filtered before use) were made until no further frequency change was observed to ensure that the sensor surface was fully covered. Electrodes thus modified were exposed to solutions of metal salts (20 μl of 0.15 M NaCl, 0.15 M KCl or 0.15 M $CaCl_2$ in aqueous solution, flow rate 5 μl min^{-1}) and resultant frequency changes monitored for up to 20 min.

Molecular Modelling

Geometry optimization calculations were carried out on **1c**·Na^+, **1c**·K^+ and **1c**·Ca^{2+} using *ab initio* (HF/3–21G(d,p)) methods (Titan, v. 1.05, Wavefunction, Irvine, CA, USA) to determine how far each cation penetrated the oxacalixarene cavity. The trajectory of guest inclusion was determined for cation–ligand complexes using molecular mechanics to simulate gas-phase interactions between Na^+ and **1c** (Spartan '04, v. 1.00, Wavefunction, Irvine, CA, USA). Initial ligand geometries for cone and partial cone conformers were constructed and optimized using the MMFF force field. In both simulations the Na^+ guest was constrained to reside at 7.500 Å from the ethereal oxygen atoms in the macrocyclic ring. This distance was reduced in 10 steps to leave the cation lying coplanar with the ethereal oxygens: for each step the ligand was allowed to adopt an optimized geometry and the energy recorded. The reported values have been corrected for the energy due to the constraints.

Mathematical Modelling of Cation Binding

The lowering of quartz crystal oscillation frequency in liquid media, as in the QCRS experiment, can be written as follows [37]:

$$\Delta f = -f_0^{1.5}\left(\frac{\eta_l \rho_l}{\pi \mu_q \rho_q}\right)^{0.5} \tag{1}$$

where Δf is the measured frequency shift, f_0 is the resonant frequency of the unloaded quartz crystal, ρ_l is the density of liquid in contact with the crystal, η_l is the viscosity of liquid in contact with the crystal, ρ_q is the specific density of quartz (2.648 g cm^{-3}) and μ_q is the shear modulus of quartz (2.947×10^{11} g cm^{-1} s^{-2}). In the case of adsorption of mass m_a in the form of a film on the crystal from a liquid, the oscillation frequency diminishes in accordance with:

$$\Delta f = -f_0^{1.5}\left(\frac{\eta_l \rho_l}{\pi \mu_q \rho_q}\right)^{0.5} - c m_a (1 - x) \tag{2}$$

where c is a constant and x is the viscous correction factor dependent on the mechanical properties of an adsorbed film and an aqueous solution [38]. If this film (with thickness h_f and specific density ρ_f) is relatively rigid and the liquid is Newtonian, the load from this layer and the liquid load are approximately additive [39]:

$$\Delta f = -f_0^{1.5}\left(\frac{\eta_l \rho_l}{\pi \mu_q \rho_q}\right)^{0.5} - \frac{2 f_0^2 \rho_f h_f}{(\mu_q \rho_q)^{0.5}}. \tag{3}$$

The time dependence of a portion of the $\Delta f(t)$ curve corresponding to a sharp decrease in frequency through oxacalix[3]arene adsorption to the sensor surface can be given by:

$$\ln \frac{\Delta f}{A} = -kt \tag{4}$$

where k is the pseudo-first-order adsorption rate constant. This "constant", however, decreases with time because of increasing coverage, Θ, of the sensor surface. Thus Eq. (4) can be rewritten as:

$$\Delta f = A\left\{\exp\left[-\frac{\gamma(t-\alpha)^{\nu}}{1+\beta(t-\alpha)}\right] - 1\right\} \tag{5}$$

where α is a constant corresponding to the time between a compound's addition to the liquid flow and the beginning of its adsorption onto the sensor surface; β, γ and ν are the equation parameters (dependent on the compound concentration, sensor and liquid characteristics, temperature, etc.); $\exp[\,] < 1$; $\nu > 1$; and $A \approx -\Delta f_m$ is a maximal change due to the adsorption. Parameters β, γ and ν can be determined by solving Eq. (6):

$$\Phi(\alpha,\beta,\gamma,\nu) = \int_{t_{min}}^{t_{max}} \left\{ spline(\Delta f_{exp}(t)) - A\left[\exp\left(-\frac{\gamma(t-\alpha)^{\nu}}{1+\beta(t-\alpha)}\right) - 1\right]\right\}^2 dt \rightarrow \min \tag{6}$$

under conditions $\partial\Phi/\partial x_i = 0$ ($x_i = \beta$, γ and ν). Here spline($\Delta f_{\exp}(t)$) is a cubic spline of the experimental data and the values of $t_{\min}$ and $t_{\max}$ correspond to the time boundaries from the oxacalix[3]arene injection until the unbound compound is eluted from the sensor by the liquid flow. To reduce the noise influence, FFT smoothing was applied to $\Delta f_{\exp}(t)$ before minimization of the function given in Eq. (6). An equation to solve for k can then be written using Eqs. (4) and (5):

$$k = \frac{1}{t-\alpha} \ln\left\{\exp\left[-\frac{\gamma(t-\alpha)^{\nu}}{1+\beta(t-\alpha)}\right] - 1\right\} \qquad (7)$$

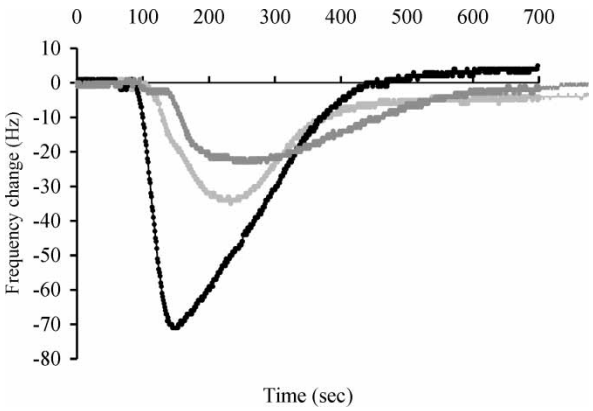

FIGURE 3 QCRS trace comparing interactions between **1c** and Na^+ (black), K^+ (light grey) or Ca^{2+} (dark grey) injected at 0 s in parallel experiments.

DISCUSSION

Aqueous solutions of oxacalix[3]arenes **1a** and **1b** were passed over self-assembled monolayers (SAMs) of 11-mercaptoundecanoic acid on gold-plated quartz crystals until saturation established a stable base frequency. Our attempt to bind **1b** was unsuccessful presumably because the ethyl groups on the lower rim had little electrostatic affinity for the acid termini of the SAM. We therefore prepared the oxacalix[3]-arene ester **1c**, which was expected to have improved aqueous solubility over **1a** and an increased likelihood of attracting cations to the macrocyclic cavity, and tested it to give a comparison with **1a**. We report full synthetic details for **1c** and its precursor, ethyl 3,5-bis(hydroxymethyl)-4-hydroxybenzoate, as we have found the literature methods to be unreliable [34,35].

The QCRS results for **1a** (Fig. 2) indicate that the frequency change upon Na^+ binding is more than double that for K^+ under the same conditions; however, both cations are bound, and released, slowly. By contrast, cation interactions with **1c** (Fig. 3) show rapid binding, followed by slower release, of Na^+ compared to K^+ and Ca^{2+}. Given that the residence time within the flow cell for the 20-μl aliquots of metal chlorides is approximately 240 s, all three of the cations are retained slightly longer than expected. It is important to note that the magnitude of the frequency changes upon Na^+ binding are, again, more than twice that observed for K^+ or Ca^{2+}. Assuming that the sensor surface coverage by **1c** is approximately the same as **1a**, the data imply that when the *t*-butyl group of **1a** is replaced by the ester in **1c** the strength and specificity of Na^+ binding are enhanced. As a control, aqueous solutions of metal chlorides were passed over the SAM in the absence of oxacalix[3]arenes and no significant binding was observed.

The QCRS profiles comprise two events: binding by the guest cation followed by its release. Although rates of desorption are difficult to quantify, it is possible to model the rates of adsorption and relate these to the affinities of the oxacalix[3]arenes for the three metals.

Estimation of the contribution to the frequency change from the surface-modified quartz crystal alone when placed in a flowing solvent, assuming that the viscosity and density of the oxacalix[3]arene solutions are within 1% of the pure solvent, gives $-\Delta f < 20$ Hz. As the systems studied have a $-\Delta f$ shift close to or greater than 20 Hz (the smallest shift is approximately 16 Hz for **1a** with K^+), adsorption of the cations is deemed to have occurred in each case.

Analysis of k against reduced time ($t - \alpha$) (Fig. 4) shows a marked difference in the adsorption rate for approximately 10 s after the time of initial interaction. Thus adsorption occurs rapidly as the cations enter the QCRS flow chamber. This result is in agreement with the estimation of diminution of frequency due to changes in the liquid characteristics (η_l, ρ_l) and the concomitant drop in adsorption. In the case of **1a** a greater initial adsorption rate is observed for the complex with K^+ but for **1c** the complex with Na^+ shows a higher k value. Similar results are observed for $d(\Delta f(t))/dt$ calculated for complexes **1c** with all

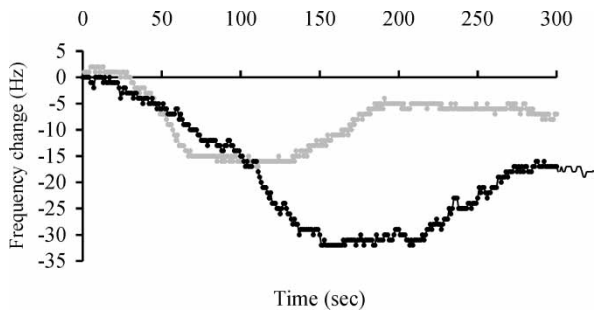

FIGURE 2 QCRS trace comparing interactions between **1a** and Na^+ (black) or K^+ (light grey) injected at 0 s in parallel experiments.

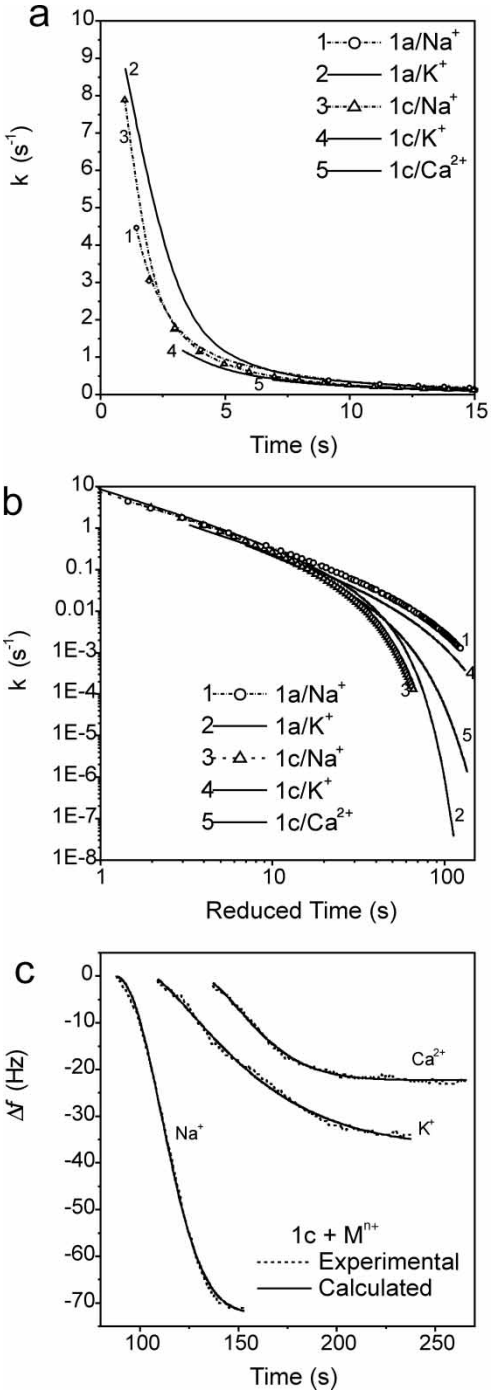

FIGURE 4 Kinetic coefficient k as a function of (a) time, (b) reduced time ($t - \alpha$), and (c) fitting of experimental $\Delta f_{exp}(t)$ using Eq. (6).

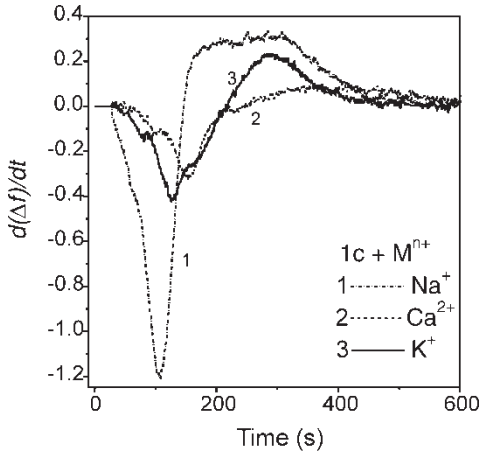

FIGURE 5 Derivatives $d(\Delta f(t))/dt$ for complexes of **1c** with Na^+, K^+ and Ca^{2+}.

the cations studied (Fig. 5): the adsorption of Na^+ by **1c** is significantly faster than the others.

To further explore factors behind the preference for Na^+ over K^+ and Ca^{2+} we used molecular simulations of cation interactions with **1c**. For the sake of simplicity gas-phase interactions were simulated as our interest was in the final positions occupied by the cavity-bound cations and not the influence of the solvent. In most crystal structures of solvated oxacalix[3]arene–metal complexes the solvent molecules do not compete for the cavity [40–43]. Our approach therefore allows us to use appropriate models (molecular mechanics, semi-empirical or *ab initio*) for the simulations without requiring extensive, or time-consuming, computational provision. The results reveal that, of the three metals, Na^+ is drawn into the cavity to the greatest extent and is positioned off-centre. Although other ions have some closer interactions with the aromatic groups or the ethereal oxygens, the excellent complementarity between the macrocyclic cavity and Na^+ mirrors the strong yet reversible binding detected by the QCRS. The data in Table I indicate that K^+, occupying a central position in the cavity, lies too far above the ethereal plane for the oxygens to have a significant interaction, although the aromatic rings may have some influence. This is consistent with the QCRS result that shows **1c** binding to K^+ with a small transient change in resonant frequency. Ca^{2+} enters more deeply into the macrocyclic cavity but the cation–π interactions appear to be weaker. The similarity in size between Ca^{2+} and Na^+ would seem to be the determining factor in its binding and the higher charge density responsible for the slow rate of release (500 s from binding to complete return to baseline compared to 430 s for Na^+ in Fig. 3). Although it gives rise to a very

TABLE I Calculated **1c**–metal interactions (Å)

	Na^+	K^+	Ca^{2+}
Ether O_1	2.86(4)	2.93(5)	2.78(5)
Ether O_2	2.94(1)	2.94(5)	2.71(8)
Ether O_3	2.74(9)	2.91(1)	2.75(4)
Centroid a	4.08(8)	3.77(2)	3.93(3)
Centroid b	3.96(1)	3.93(7)	4.03(9)
Centroid c	3.81(0)	3.85(5)	3.96(0)
Plane (O_1–O_2–O_3)	−0.186	+0.442	−0.089

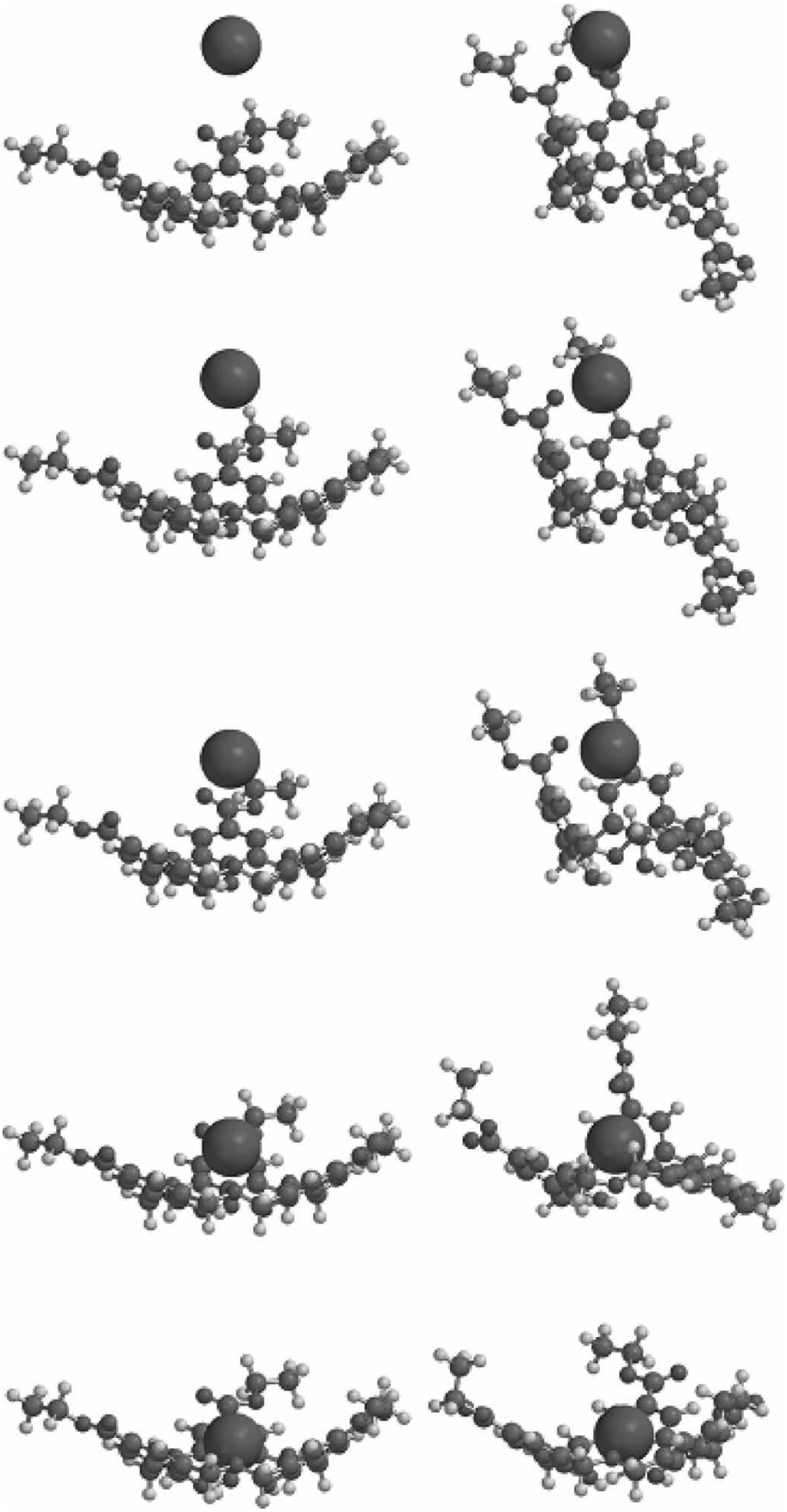

FIGURE 6 Snapshots of simulated dynamic models for **1c**–Na^+ complexation by cone (left) and partial cone (right) conformers.

small frequency change upon binding, once the Ca^{2+} complex has been formed, the metal appears to be difficult to remove.

A final problem exists with the formation of oxacalix[3]arene inclusion complexes under these conditions. Oxacalix[3]arenes, in common with other calix[*n*]arenes, may adopt more than one conformation but, unlike other calix[*n*]arenes, only two conformers, cone and partial cone, exist. In the former, the three aromatic rings have the same orientation and are stabilized by a hydrogen-bonding network involving the three phenolic protons. In the latter, one aromatic ring is inverted with respect to the other two. To bind cations the macrocycles must adopt a cone conformation as the central cavity within the partial cone conformers tends to collapse, making cation inclusion difficult, if not impossible [15]. Statistically, in solution, only 25% of the uncomplexed oxacalix[3]arene hosts will adopt the cone conformer at any one time [33]; thus when preparing SAMs that incorporate oxacalix[3]arenes, the majority of the molecules will not be preorganized to bind guests. To determine whether approaching cations could influence the cone–partial cone equilibrium, a model for adsorption was developed. Molecular simulations (Fig. 6) illustrate the attraction of Na^+ to the central cavity of **1c**. Regardless of the initial geometry, cone or partial cone, the final complex always adopts the cone conformer. The implication of this dynamic model is that **1c** need not initially adsorb onto the quartz crystal SAM in a cone conformer to ensure subsequent cation binding. Analysis of the trajectory by which the cation approaches the binding site reveals that Na^+ approaches the cavity of the cone conformer gradually and reduces the overall steric energy to the point of optimum binding. By way of contrast, the approach of the cation to the partial cone has little influence on the overall energy of the complex until it is able to force the macrocycle to adopt a cone conformer. From that point forward in the simulation the trajectory shadows that of the Na^+–cone complex, as illustrated in Fig. 7. Fully solvated models may give a more accurate description of this behaviour; however, these molecular mechanics simulations give a strong indication of the general mechanism by which cations can influence the geometry of the macrocycle to give optimum binding.

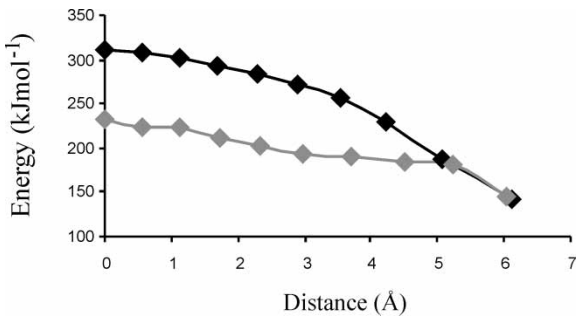

FIGURE 7 Cation binding trajectories for cone–**1c** (black) and partial cone–**1c** (grey) with Na^+. Distances are given from the cation's initial position above the plane described by the ethereal oxygens.

In conclusion, we have demonstrated that transient binding events occurring between alkali or alkaline earth metals and oxacalix[3]arenes can be observed in real-time using the quartz crystal resonant sensor. This technique may have widespread applications as a method to study transient binding events not observable by NMR, crystallographic or extraction studies. The results obtained are consistent with both computational models for the rates of initial binding and molecular simulations of putative metal–oxacalix[3]arene complexes formed thereafter.

Acknowledgements

This work was supported by the EPSRC (GR/N35229, GR/P00123), the Royal Society (short-term visits by V.M.G.) and the Sussex High Performance Computing Initiative. The assistance of Dr F. Paul is gratefully acknowledged.

References

[1] Andreeti, G. D.; Ungaro, R.; Pochini, A. J. *J. Chem. Soc., Chem. Commun.* **1979**, 1005–1006.
[2] Harrowfield, J. M.; Ogden, M. I.; Richmond, W. R.; White, A. H. *J. Chem. Soc., Chem. Commun.* **1991**, 1159–1160.
[3] Atwood, J. L.; Hamada, F.; Robinson, K. D.; Orr, G. W.; Vincent, R. L. *Nature* **1991**, *349*, 683–684.
[4] MacGillivray, L. R.; Atwood, J. L. *Nature* **1997**, *389*, 469–472.
[5] Atwood, J. L.; Barbour, L. J.; Jerga, A. *J. Am. Chem. Soc.* **2002**, *124*, 2122–2123.
[6] Orr, G. W.; Barbour, L. J.; Atwood, J. L. *Science* **1999**, *285*, 1049–1052.
[7] Diamond, D.; Nolan, K. *Anal. Chem.* **2001**, 23A–29A.
[8] Molenveld, P.; Engbersen, J. F. J.; Reinhoudt, D. N. *Chem. Soc. Rev.* **2000**, *29*, 75–86.
[9] Hultzsch, K. *Kunststoffe* **1962**, *52*, 19–24.
[10] Dhawan, B.; Gutsche, C. D. *J. Org. Chem.* **1983**, *48*, 1536–1539.
[11] Araki, K.; Hashimoto, N.; Otsuka, H.; Shinkai, S. *J. Org. Chem.* **1993**, *58*, 5958–5963.
[12] Hampton, P. D.; Daitch, C. E.; Duesler, E. M. *New J. Chem.* **1996**, *20*, 427–432.
[13] Tsubaki, K.; Otsubo, T.; Tanaka, K.; Fuji, K.; Kinoshita, T. *J. Org. Chem.* **1998**, *63*, 3260–3265.
[14] Ohkanda, J.; Shibui, H.; Katoh, A. *Chem. Commun.* **1998**, 375–376.
[15] Cragg, P. J.; Drew, M. G. B.; Steed, J. W. *Supramol. Chem.* **1999**, *11*, 5–15.
[16] Ikeda, A.; Sonoda, K.; Shinkai, S. *Chem. Lett.* **2000**, 1220–1221.
[17] Hampton, P. D.; Daitch, C. E.; Alam, T. M.; Pruss, E. A. *Inorg. Chem.* **1997**, *36*, 2879–2883.
[18] Tsubaki, K.; Tanaka, K.; Kinoshita, T.; Fuji, K. *Chem. Commun.* **1998**, 895–896.
[19] Atwood, J. L.; Barbour, L. J.; Nichols, P. J.; Raston, C. L.; Sandoval, C. A. *Chem. Eur. J.* **1999**, *5*, 990–996.
[20] Masci, B. *Tetrahedron* **1995**, *51*, 5459–5464.
[21] Hampton, P. D.; Bencze, Z.; Tong, W.; Daitch, C. E. *J. Org. Chem.* **1994**, *59*, 4838–4843.
[22] Cragg, P. J.; Allen, M. C.; Steed, J. W. *Chem. Commun.* **1999**, 553–554.

[23] Wolf, N. J.; Georgiev, E. M.; Yordanov, B. R.; Whittlesey, B. R.; Koch, H. F.; Roundhill, D. M. *Polyhedron* **1999**, *18*, 885–896.
[24] Arduini, A.; Giorgi, G.; Pochini, A.; Secchi, A.; Ugozzoli, F. *Tetrahedron* **2001**, *57*, 2411–2417.
[25] Moser, A.; Yap, G. P. A.; Detellier, C. *J. Chem. Soc., Dalton Trans.* **2002**, 428–434.
[26] Cragg, P. J.; Miah, M.; Steed, J. W. *Supramol. Chem.* **2002**, *14*, 75–78.
[27] Fucassi, F.; Pavey, K. D.; Lowe, J. E.; Olliff, C. J.; Green, M. H. L.; Paul, F.; Cragg, P. J. *Chem. Commun.* **2001**, 841–842.
[28] Pavey, K. D.; Miah, M.; Fucassi, F.; Paul, F.; Cragg, P. *J. Chem. Commun.* **2001**, 1886–1887.
[29] Pavey, K. D.; Olliff, C. J.; Paul, F. *Analyst* **2001**, *126*, 1711–1715.
[30] Patel, R.; Zhou, R. N.; Zinszer, K.; Josse, F.; Cernosek, R. *Anal. Chem.* **2000**, *72*, 4888–4898.
[31] Shana, Z. A.; Josse, F. *Anal. Chem.* **1994**, *66*, 1955–1964.
[32] Miah, M.; Romanov, N. N.; Cragg, P. J. *J. Org. Chem.* **2002**, *67*, 3124–3126.
[33] Matsumoto, H.; Nishio, S.; Takeshita, M.; Shinkai, S. *Tetrahedron* **1995**, *51*, 4647–4654.
[34] Zinke, K.; Ott, R.; Leggewie, E.; Hassanein, A.; Zankl, G. *Monatsh. Chem.* **1956**, *87*, 552–559.
[35] Zhong, Z.; Ikeda, A.; Shinkai, S. *J. Am. Chem. Soc.* **1999**, *121*, 11906–11907.
[36] Bain, C. D.; Troughton, E. B.; Tao, Y.-T.; Evall, J.; Whitesides, G. M. *J. Am. Chem. Soc.* **1989**, *111*, 321–335.
[37] Kanazawa, K. K.; Gordon, J., II *Anal. Chem.* **1985**, *57*, 1770–1771.
[38] Voinova, M. V.; Jonson, M.; Kasemo, B. *Biosens. Bioelectron.* **2002**, *17*, 835–841.
[39] Lucklum, R.; Hauptmann, P. *Electrochim. Acta* **2000**, *45*, 3907–3916.
[40] Daitch, C. E.; Hampton, P. D.; Duesler, E. N.; Alam, T. M. *J. Am. Chem. Soc.* **1996**, *118*, 7769–7773.
[41] Thuery, P.; Nierlich, M.; Masci, B.; Asfari, Z.; Vicens, J. *Dalton Trans.* **1999**, 3151–3152.
[42] Masci, B.; Nierlich, M.; Thuery, P. *New J. Chem.* **2002**, *26*, 120–128.
[43] Masci, B.; Nierlich, M.; Thuery, P. *New J. Chem.* **2002**, *26*, 763–774.